of the Physical Society of Japan
, No. 4, April, 1990, pp. 1218–1224

Charge Transfer Cross Sections of $^3He^{2+}$ Ions in Collisions with He Atoms and H_2 Molecules in the Energy Range of 1 ~ 10 keV

Toshio KUSAKABE, Hiroshi YONEDA, Yoshihiko MIZUMOTO and Kousuke KATSURAYAMA

Department of Nuclear Reactor Engineering, Faculty of Science and Technology, Kinki University, Kowakae, Higashi-osaka, Osaka 577

(Received September 29, 1989)

The single- and double-charge transfer cross sections of $^3He^{2+}$ ions have been measured for targets of He atoms and H_2 molecules in the energy range from 1 to 10 keV by using a microchannel plate-position sensitive detector. The present results are compared with those from other experiments and with available theoretical calculations.

[single-charge transfer cross sections, double-charge transfer cross sections, $^3He^{2+}$ ions, keV energy, He target, H_2 target, position sensitive detector]

roduction

naked helium ion, He^{2+}, is one of the particles, its collision behaviors affect lds of atomic and molecular physics, sics, chemical physics, radiation nd so on. In recent years, the charge processes at energies below 100 keV ome more important in connection controlled thermonuclear fusion)

er to understand the behaviors of ns and particles produced in a fusion it is necessary to measure the single- ble-charge transfer cross sections, σ_{21} and σ_{20} respectively, by He^{2+} ions nd H_2 targets at wide energy range. ocesses at low energies would play an nt role in the edge plasma of low tem- .

authors have measured these cross sec- stly at energies above 10 keV. In the He target, Afrosimov *et al.*[2] and *et al.*[3] have presented the measured the cross sections at energies below which the theoretical calculations n performed by several authors. But sults somewhat deviate from one In the case of H_2 target, the σ_{21} values of Nutt *et al.*[4] decrease with decreasing impact energy and a deviation is found from those of Afrosimov *et al.*[5] On the other hand, the σ_{20} results measured by Afrosimov's group[5] have two maxima at about 3 and 80 keV, and cannot be connected with those of Shah and Gilbody.[6] In particular, a set of σ_{21} and σ_{20} values for H_2 target has never been reported in the low energy range.

Therefore, we present in this paper the single- and double-charge transfer cross sections for $^3He^{2+}$ ions on He and H_2 in the energy range from 1 to 10 keV. The data are compared with the existing experimental values and theoretical calculations.

§2. Experimental

The present experimental apparatus and methods are similar to those of Kyoto University's group[7] and have been described in detail elsewhere.[3] Therefore only the main features are briefly mentioned here.

The experimental arrangement is schematically shown in Fig. 1. A He^{2+} ion beam was extracted from an electron impact ion source. In order to avoid contamination of the beam by H_2^+ impurity ions, ^3He gas was supplied to the ion source. The beam analyzed in a Wien filter was introduced into a 40 mm long

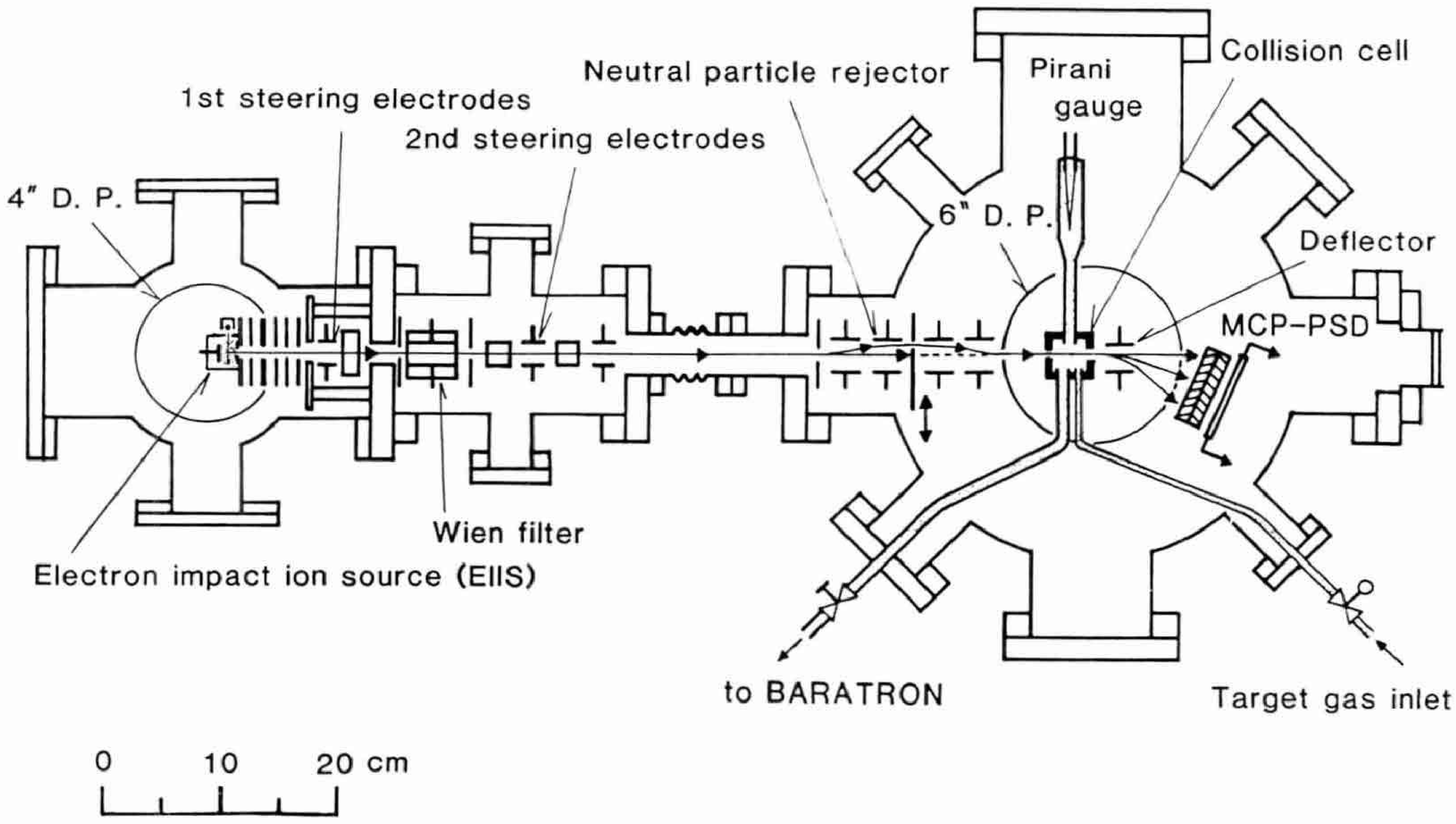

Fig. 1. Schematic diagram of the experimental arrangement.

collision cell having a 0.5 mm$^\phi$ entrance and 3.5 mm$^\phi$ exit apertures. Target gas of He and H_2 with high purity (>99.999%) was fed into the cell and the gas pressure was monitored with the use of a sensitive Pirani gauge which had been calibrated by a capacitance manometer (MKS-BARATRON 590HA-00001). The outgoing ions from the cell were electrostatically deflected by a parallel plate and impinged onto the surface of an MCP-PSD, which was made of a rectangular (46 mm × 13 mm) tandem microchannel plate with a resistive anode of a few kΩ. The output signals from both ends of the resistive anode were processed in an analog circuit in order to obtain a position signal with a wide dynamic range of 50 mV ~ 10 V.[8] The position signals were recorded on a pulse height analyzer (PHA: Canberra MCA35+) to display a charge spectrum of He^{2+}, He^+ and He^0 events.

The values of the charge transfer cross sections were derived by applying a growth rate method. From each net peak area the charge fractions, F_{21} and F_{20}, were obtained as a function of target thickness π in the range from 0.21 ~ 4.3 Pa·cm, and the σ_{2j} values ($j=1$ and 2) were derived by fitting these fractions to the following equation:

$$F_{2j} \simeq \sigma_{2j} \cdot \pi + C_j \cdot \pi^2, \qquad (1)$$

where C_j is a coefficient including several cross sections.

The statistical deviations of σ_{2j} values are typically ranging from a few % to 9.6% ($j=2$ for H_2 target at 10.0 keV). Total systematic uncertainty, such as determination of target thickness, temperature and so forth, is estimated to be 10.5% in the present work. The total experimental uncertainties for absolute values of the cross section were obtained by the quadrature sum of these uncertainties. An ambiguous factor can be given for the σ_{21} values in He^{2+}–He collisions at energies below 2.0 keV. The separation of He^+ peak on the position spectrum does not become clear as mentioned later. But the uncertainty due to this bad separation was not included into total experimental uncertainties.

§3. Results and Discussion

The present charge transfer cross sections are given in Table I. These are also depicted in Figs. 2 and 4 as a function of $^3He^{2+}$ energy. The experimental and theoretical values obtained by other research workers are inserted into these figures for the sake of comparison where the $^4He^{2+}$ energy is multiplied by 3/4 in order to fit with the energy scale for $^3He^{2+}$ ions.

Table I. Single- and double-charge transfer cross sections for 1.0~10.0 keV $^3He^{2+}$ ions on He and H_2 targets.

Target	$^3He^{2+}$ Energy (keV)	Cross sections ($\times 10^{-17}$ cm^2)	
		σ_{21}	σ_{20}
He	1.0	1.84±0.21	22.6±2.4
	1.5	3.08±0.37	22.6±2.4
	2.0	3.01±0.33	22.9±2.4
	3.0	4.06±0.44	22.4±2.4
	4.0	4.48±0.49	21.7±2.3
	6.0	5.49±0.62	20.3±2.2
	8.0	5.82±0.64	19.5±2.1
	10.0	6.01±0.64	19.1±2.0
H_2	1.0	23.1±2.5	4.23±0.47
	1.5	24.7±2.6	4.36±0.47
	2.0	24.6±2.7	4.46±0.49
	3.0	22.1±2.4	4.00±0.44
	4.0	24.0±2.5	3.69±0.40
	6.0	25.8±2.7	2.38±0.26
	8.0	28.9±3.1	1.89±0.20
	10.0	32.8±3.5	1.18±0.17

3.1 He target

The single-charge transfer cross sections, σ_{21}, for He^{2+} ions on He are plotted in the lower half of Fig. 2. The observations by others[9-12] at more than 10 keV in energy are also indicated. The present σ_{21} data, which are consistent with our preliminary experiment[3] on $^4He^{2+}$-He collision, are about twice as large as the results of Hertel and Koski[13] and monotonously increase with increasing incident energy. Our values can be connected with the higher energy data of Berkner *et al.*[9] and Bayfield and Khayrallah.[11]

The cross section curve measured by Afrosimov *et al.*[2] has a minimum at about 7 keV. They have also reported that the observed differential cross sections for the charge transferred He^+ ions can be divided into two parts—charge transfers to the state with principal quantum number $n=2$ and to that with $n \geqq 3$. As shown in Fig. 3, we have also observed that the width of the product He^+ peak

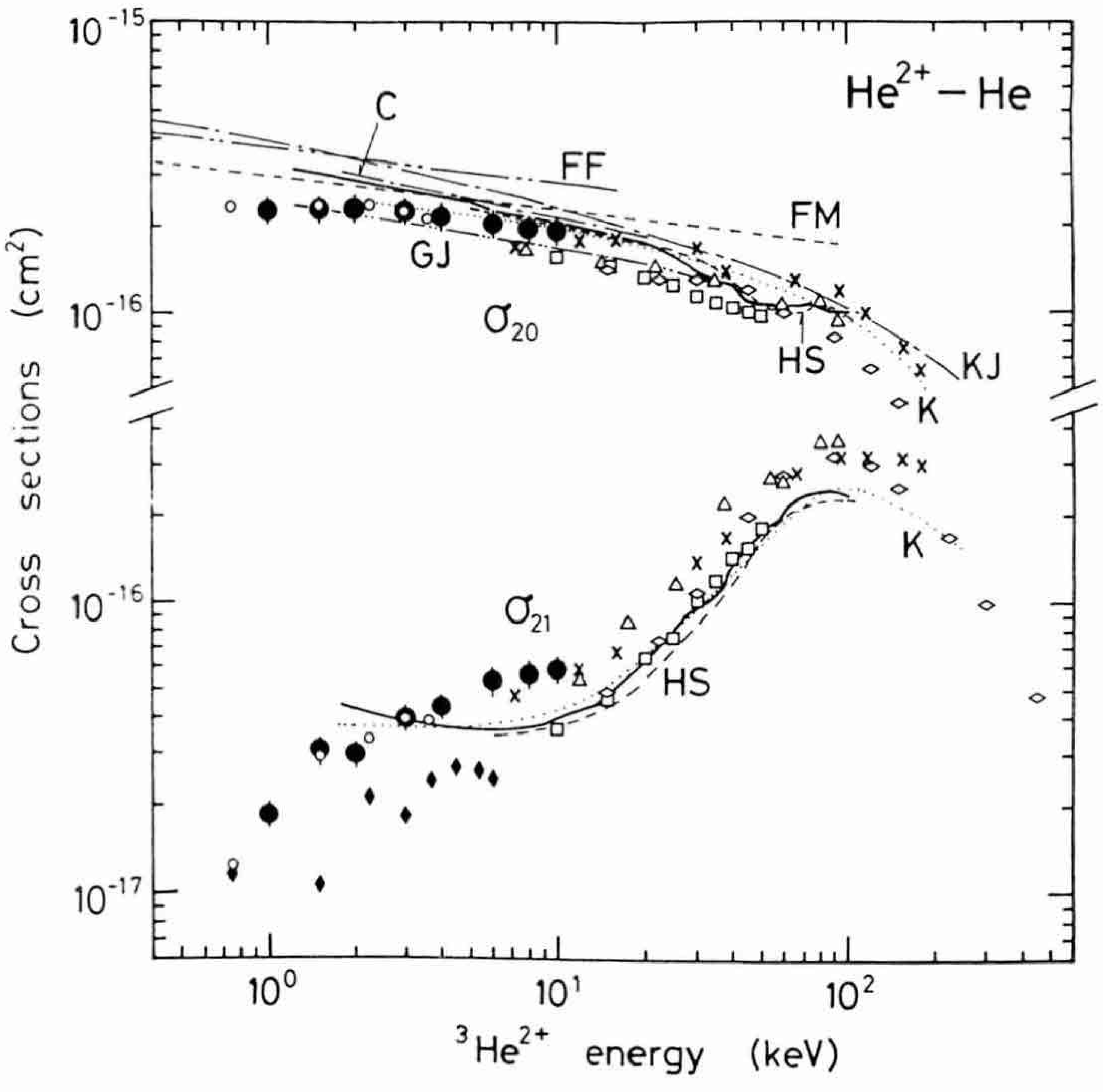

Fig. 2. Single- and double-charge transfer cross sections, σ_{21} and σ_{20}, respectively, for He^{2+} ions on He as a function of $^3He^{2+}$ energy. Experimental data: ●-Present data, ○-Kusakabe *et al.* (1988),[3] ◇-Rudd *et al.* (1985),[12] —-Afrosimov *et al.* (1975),[2] △-Bayfield and Khayrallah (1975),[11] □-Shah and Gilbody (1974),[10] ×-Berkner *et al.* (1968),[9] ◆-Hertel and Koski (1964).[13] Theory: K-Kimura (1988),[15] HS-Harel and Salin (1980),[14] GJ-Grozdanov and Janev (1980),[23] C-Chibisov (1976),[19] KJ-Komarov and Janev (1967),[18] FF-Fetisov and Firsov (1960),[17] FM-Ferguson and Moiseiwitsch (1959).[16]

on the position spectrum spreads with decreasing projectile energy and its peak profile has the structure which may be related to the mechanism of the single-charge transfer reaction in He^{2+}–He collision system. Although the separation of He^+ peak area becomes ambiguous at energies below 2 keV, our σ_{21} data have no minimum up to 10 keV in energy and is in contradiction with Afrosimov's.

The comparable theoretical σ_{21} values are of Harel and Salin[14] and Kimura,[15] but these disagree with our observations. This discrepancy cannot be clearly explained at present. For "single-charge transfer" in the He^{2+}–He collision, the following processes would occure:

$$He^{2+} + He \rightarrow He^+ + He^+ \text{ ("pure" single-charge transfer)} \quad (2)$$

$$\rightarrow He^+ + He^{2+} + e^- \text{ (transfer and ionization of target atom)} \quad (3)$$

$$\rightarrow He^{0**} + He^{2+} \text{ (autoionization after double-charge transfer)} \quad (4)$$

$$\hookrightarrow He^+ + e^-.$$

It should be noted that the processes (3) and (4) are not taken into account in their theoretical calculations.

The double-charge transfer cross sections, σ_{20}, are represented in the upper half of Fig. 2 together with other data and the typical theorical curves. Since this collision is "symmetric resonant charge transfer" as

$$He^{2+} + He \rightarrow He^0 + He^{2+} \text{ (double-charge transfer),} \quad (5)$$

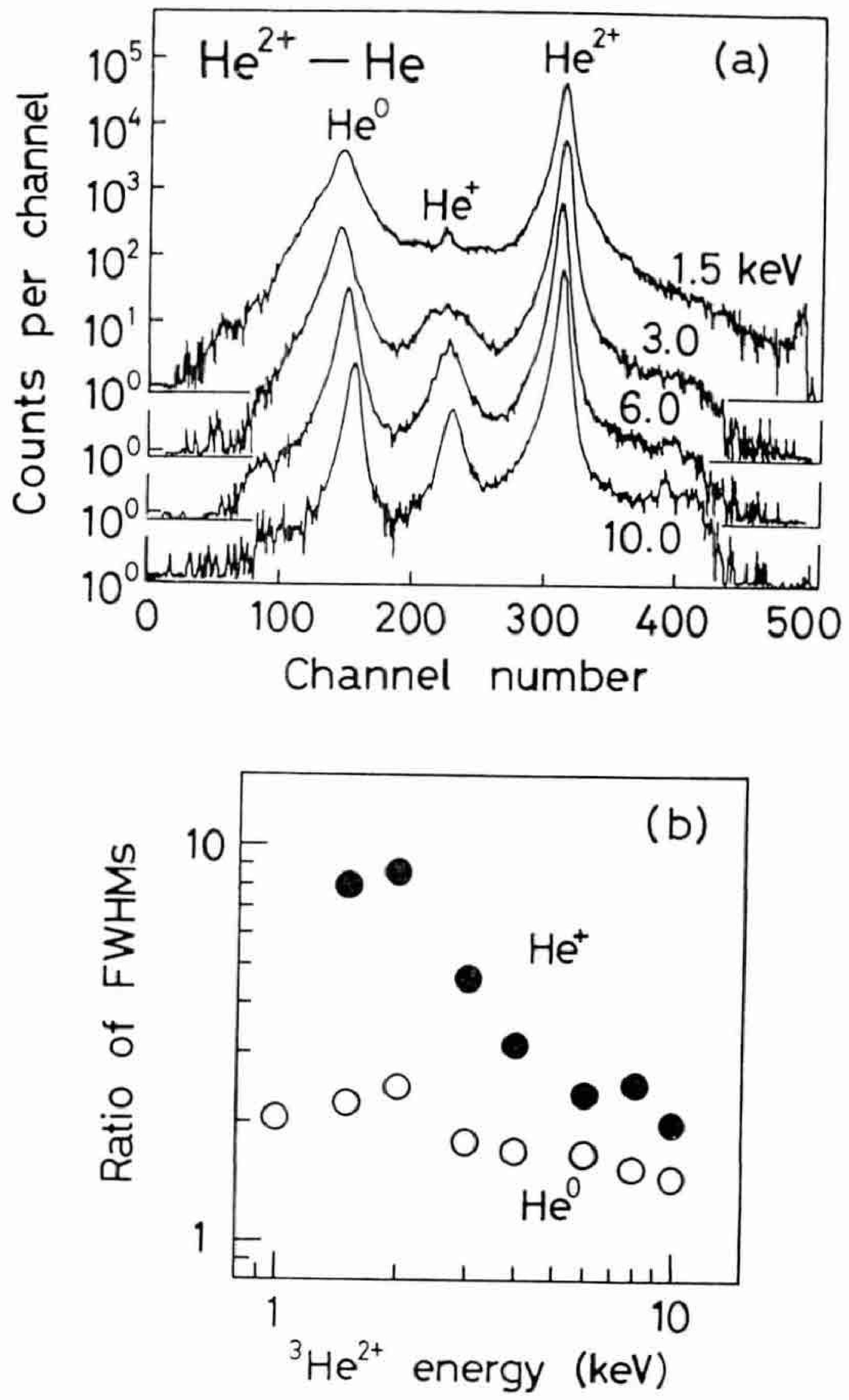

Fig. 3. Variation of the peak width of charge transferred helium ions in $^3He^{2+}$–He collision. (a) Typical position (charge) spectra at 1.5, 3.0, 6.0 and 10.0 keV in energy. The target thicknesses of helium gas were 2.6 to 0.8×10^{-2} Torr·cm. (b) Ratio of full width at half maximum (FWHM) for the peak of charge transferred ions to that for primary He^{2+} ions as a function of $^3He^{2+}$ energy. Solid and open circles correspond to the He^+ and He^0 peaks, respectively.

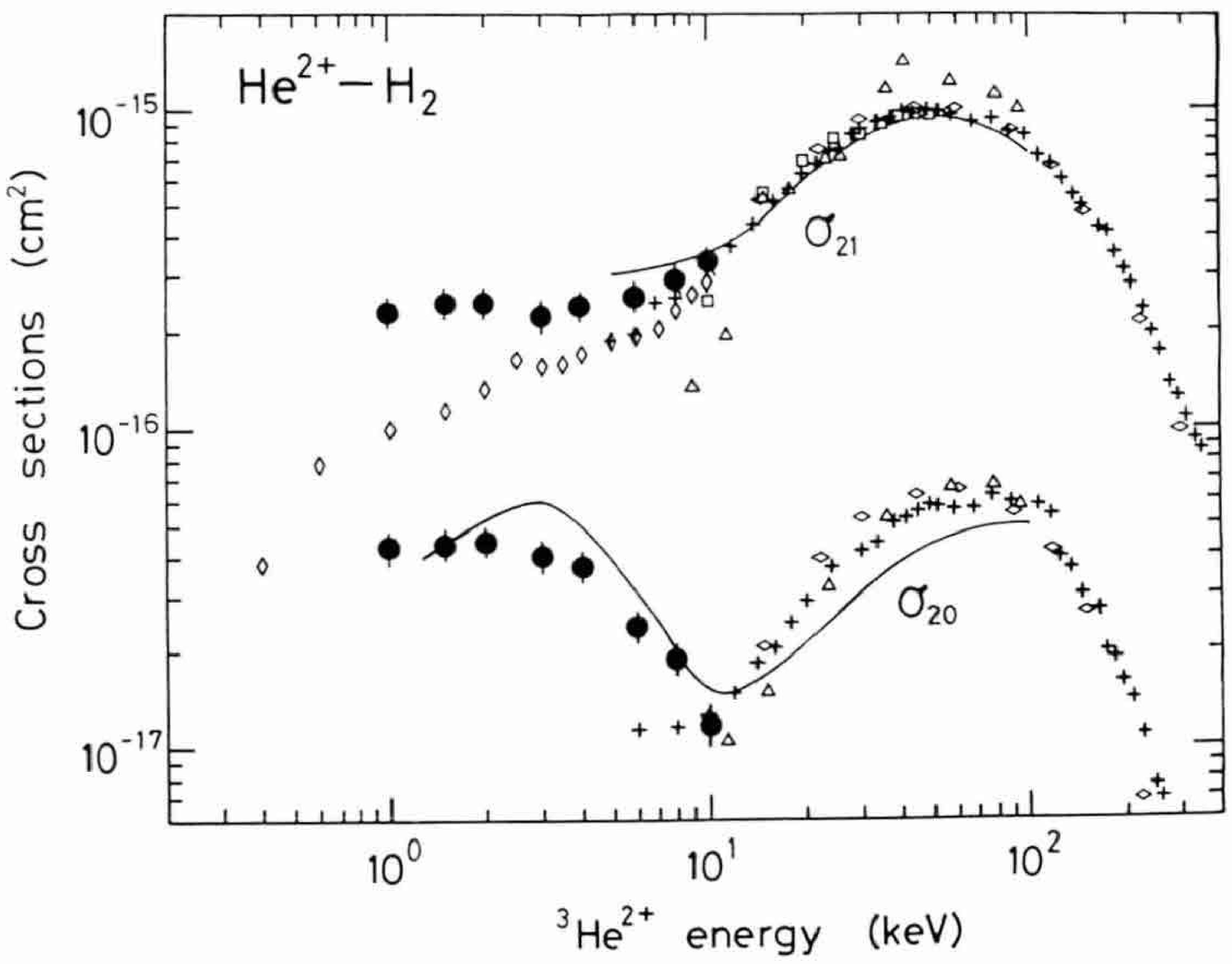

Fig. 4. Single- and double-charge transfer cross sections, σ_{21} and σ_{20}, respectively, for He^{2+} ions on H$_2$ as a function of ^{3}He^{2+} energy. Experimental data: ●-Present data, ◇-Rudd *et al.* (1985),[12] ◇-Nutt *et al.* (1978),[4] —-Afrosimov *et al.* (1980),[5] +-Shah and Gilbody (1978),[6] △-Bayfield and Khayrallah (1975),[11] □-Shah and Gilbody (1974).[10]

the σ_{20} values are generally larger than the σ_{21} ones in the low energy region and gradually decrease with increasing incident He^{2+} energy. The present results are a little smaller than those of Afrosimov *et al.*,[2] but are well consistent with our previous experiment[3] and can be connected with the data of Berkner *et al.*[9] Figure 3(b) reveales that the width of He^0 peak is rather constant irrespective of the projectile energy in contrast to the He$^+$ peak in the same figure.

Nearly ten theoretical works have been presented since 1960s,[14-20] but the theoretical σ_{20} values of Harel and Salin,[14] Grozdanov and Janev[20] and Kimura[15] coincide with our data within the experimental uncertainties.

3.2 *H$_2$ target*

Figure 4 shows the single- and double-charge transfer cross sections for He^{2+} ions on H$_2$ together with the data of other workers. The theoretical treatments for this system have never been presented. Although there are several σ data at more than 10 keV of ion energy, poor observations are found in the lower energy region. In particular, no one has reported a set of the σ_{21} and σ_{20} values.

The present σ_{21} data indicate a weak dependence on ion energy and have a soft minimum at around 3 keV. These can be reasonably connected with the values of other workers[5,6,10,12] at energies above 10 keV. The results of Nutt *et al.*[4] are obviously smaller than ours and the discrepancy increases with a decrease in impact energy of He^{2+} ions.

The reason would be attributed to their instrumental feature that they could not sufficiently collected the fast product ions after charge transfer because of the very long length between the exit aperture of the gas cell and the detector (60 cm) and the small acceptance angle of the detector. Referring to the coincidence measurements with the secondary ions done by Afrosimov *et al.*,[5] the following processes represented by eqs. (6) and (7) would become dominant at energies above and below 10 keV, respectively.

$$\mathrm{He}^{2+}+\mathrm{H}_2\rightarrow\mathrm{He}^{+}+\mathrm{H}_2^{+}\ (\text{“pure” single-charge transfer}) \tag{6}$$

$$\left.\begin{aligned}&\rightarrow\mathrm{He}^{+}+\mathrm{H}^{+}+\mathrm{H}\ (\text{dissociative single-charge transfer})\\&\rightarrow\mathrm{He}^{+}+\mathrm{H}^{+}+\mathrm{H}^{+}+e^{-}\ (\text{transfer and ionization}).\end{aligned}\right\} \tag{7}$$

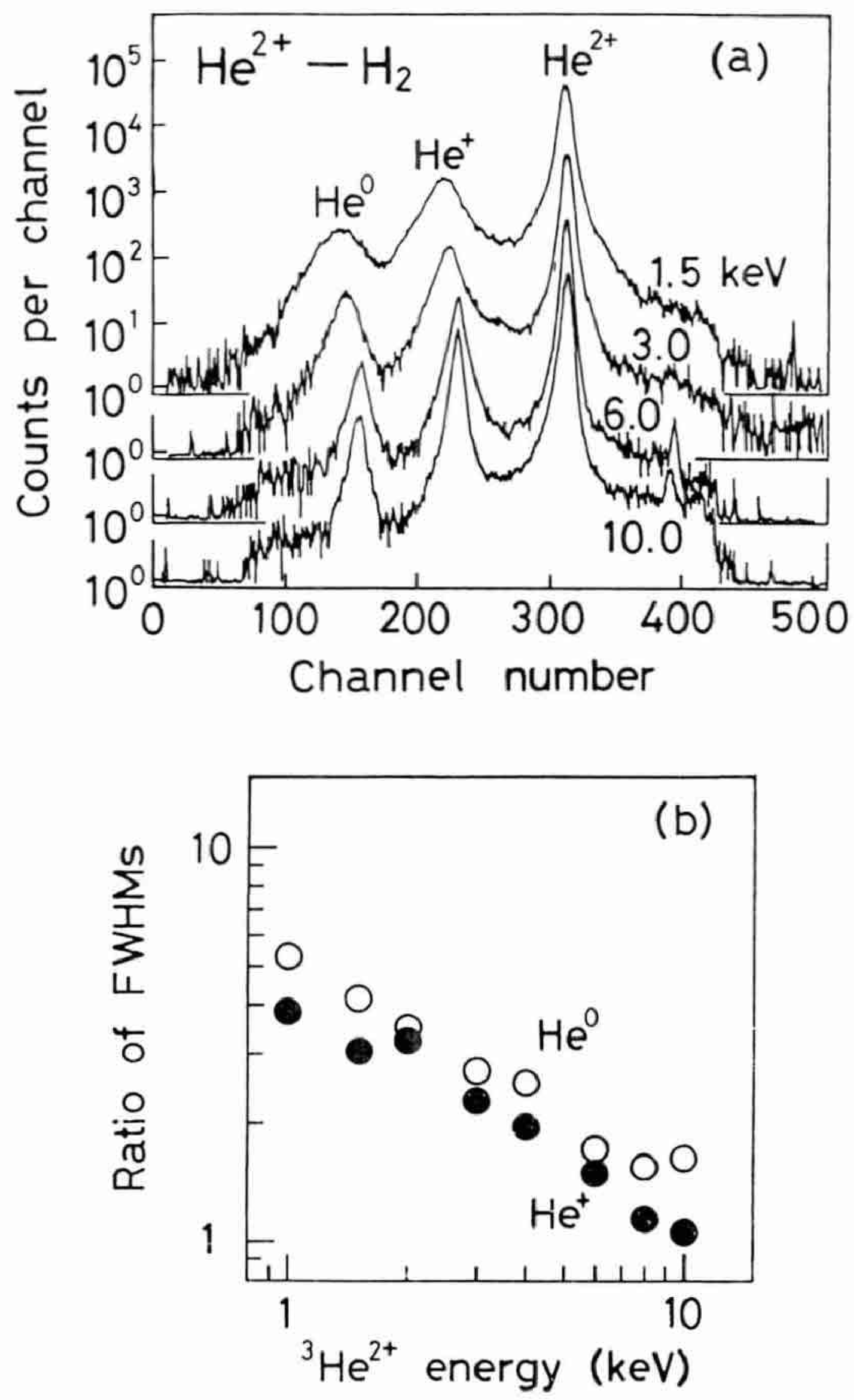

Fig. 5. Variation of the peak width of charge transferred helium ions in $^3He^{2+}$-H_2 collision. (a) Typical position (charge) spectra at 1.5, 3.0, 6.0 and 10.0 keV in energy. The target thicknesses of molecular hydrogen gas were around 1.4×10^{-2} Torr·cm. (b) Ratio of full width at half maximum (FWHM) for the peak of charge transferred ions to that for primary He^{2+} ions as a function of $^3He^{2+}$ energy. Solid and open circles correspond to the He^+ and He^0 peaks, respectively.

In the process (7), the kinetic energy of He^+ ions varies according to the ejection angles of the dissociated particles (He^+ or H), so that the He^+ ions after charge transfer scatter around their original direction. This is supported by our PSD spectra of Fig. 5 that the peak width of the He^+ ions becomes broader as the incident energy decreases. Therefore, it seems that Nutt *et al.*[4] underestimated their σ_{21} values. It is noted that they have also measured the single-charge transfer cross sections of atomic hydrogen target by He^{2+} ions. Their $\sigma_{21}(H)$ values have been obtained by the ratio of cross sections for He^+ formation in H and H_2 targets ($\sigma_{21}(H)/\sigma_{21}(H_2)$). Consequently, their $\sigma_{21}(H)$ values are seemed to also underestimate at energies below 2.5 keV.

In the case of σ_{20} measurements, there is only one comparable report of Afrosimov *et al.*,[5] which has a maximum and a minimum at 3 and 10 keV, respectively. Our σ_{20} behavior shows a similar pattern to their curve but the low energy maximum is not clear.

The double-charge transfer by He^{2+} ions with H_2 target is represented by

$$He^{2+}+H_2\rightarrow He^0+H^++H^+. \tag{8}$$

Since the target of H_2 molecule dissociates similarly to the processes (7), the width of He^0 peak also expands with decreasing impact energy as seen in Fig. 5. It is very interesting that the σ_{20} curve has a sharp minimum at 10 keV and this may be ascribable to the border of different electronic states of He^0 atom formed. In this process, one should also take account of the influence of the autoionization after double-charge transfer into doubly excited state.

3.3 Analysis by a statistical model

Sakisaka *et al.* have proposed "*statistical electron transfer model*" (SETM)[21] that some electrons in an electron cloud of a target particle are transferred to a projectile during the formation of a quasimolecule and the transfer proceeds statistically. This model has been applied to the single- to penta-electron transfers for slow Kr^{q+} (projectile charge number: $q=2\sim9$) ions on Kr. Moreover, the single- and double-charge transfers for keV He^{2+} ions on several targets[22] and for $1.5\sim12$ keV/q Ne^{q+} ($q=2\sim5$) ions on He and H_2 targets[23] have been treated by this statistical consideration.

According to this SETM, the cross section of k-electron transfer for target having two electrons is given by

$$\sigma_{qj}={}_2C_k\cdot P^k(1-P)^{2-k}\cdot\pi a_x^2,$$
$$(j=q-k:\ k=1,\ 2) \tag{9}$$

where ${}_2C_k$ is binomial coefficient and the transfer probability per electron P is assumed constant against impact parameter within an interaction range a_x. From the observed σ_{21} and σ_{20} sets, one can derive P and a_x as a func-

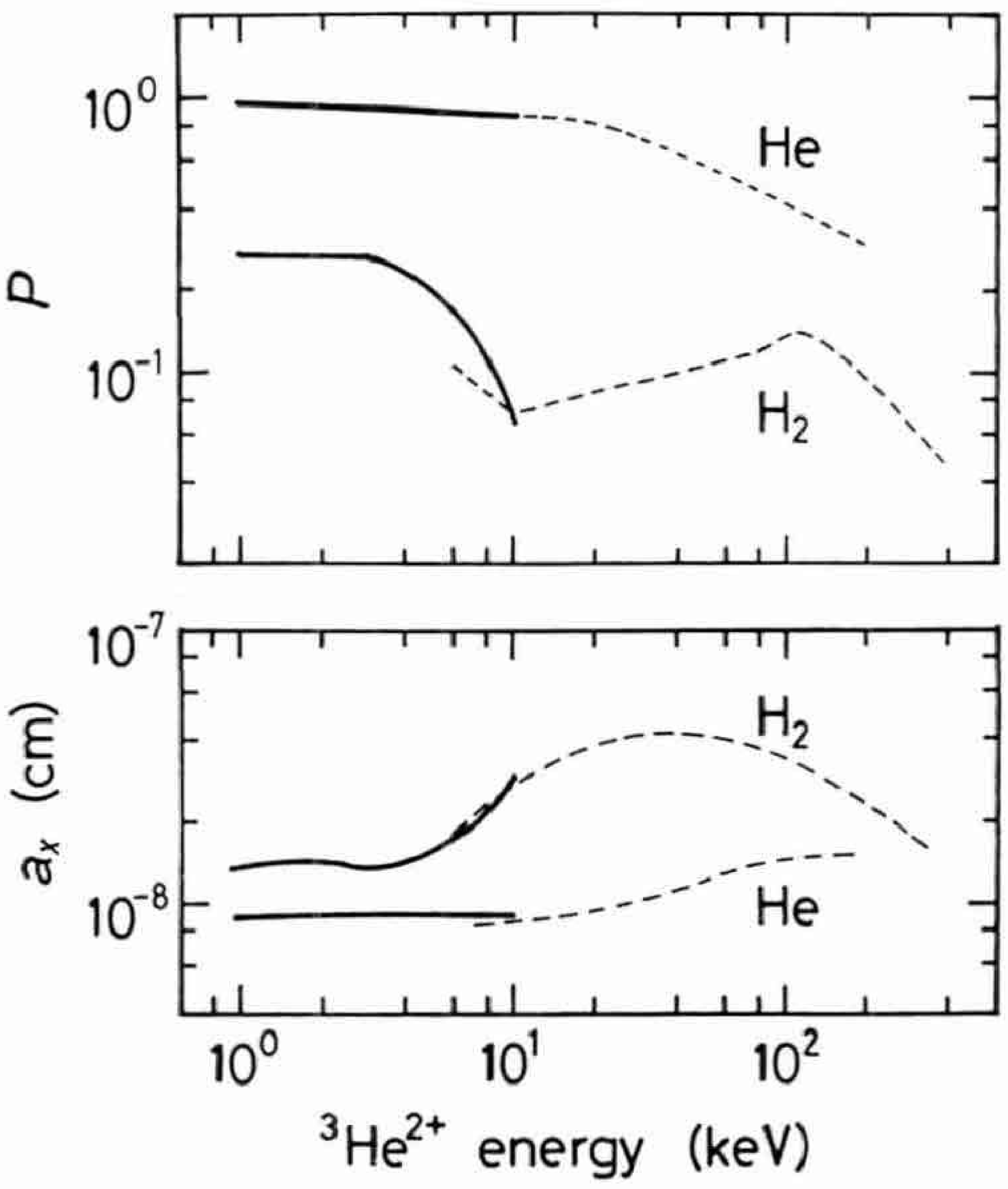

Fig. 6. Transfer probability P and interaction range a_x for He^{2+} ions on He and H_2 as a function of $^3He^{2+}$ energy. Heavy solid curves are derived from our smoothed values, whereas thin broken curves for He and H_2 targets are given referring to the data of Berkner *et al.* (1968)[9] and Shah and Gilbody (1978),[6] respectively.

tion of the projectile energy.

In Figs. 6(a) and 6(b), the P and a_x results are given by heavy solid curves, respectively. Those at higher energies are also inserted by thin broken curves. In the case of He^{2+}-He collision at energies below 10 keV, the P is as large as ~ 0.9 and the a_x, which is about thrice the radius of ground state He atom, is almost constant ($\sim 0.9 \times 10^{-8}$ cm). These mean that the electron transfer in this energy region proceeds at a large internuclear distance with a high transfer probability. As the impact energy increases, the probability decreases since the collision time becomes shorter. In the He^{2+}-H_2 collision, the P sharply gets down while the a_x grows up as the He^{2+} energy exceed 4 keV. These imply the difference of main collision processes at energies below and above 10 keV as mentioned the preceding section.

Acknowledgements

The authors would like to express sincere gratitude to Professor M. Sakisaka, Dr. M. Tomita and Mr. K. Norizawa for their useful comments and valuable suggestions. We are also appreciated to Messers A. Shigeta and S. Teraoka for their cooperative works. This work was partially supported by a Grand-in-Aid for Encouragement of Young Scientists from the Ministry of Education, Science and Culture.

References

1) H. Tawara and R. A. Phaneuf: Comm. At. Mol. Phys. **11** (1988) 177.
2) V. V. Afrosimov, G. A. Leiko, Yu. A. Mamaev and M. N. Panov: Sov. Phys.-JETP **40** (1975) 661.
3) T. Kusakabe, K. Kajiwara, K. Ohishi, K. Tsujimaru, K. Tominaga, K. Yamashita, Y. Sugimoto, S. Hayashida, Y. Mizumoto and K. Katsurayama: J. Fac. Sci. Technol. Kinki Univ. **24** (1988) 257.
4) W. L. Nutt, R. W. McCullough, K. Brady, M. B. Shah and H. B. Gilbody: J. Phys. B: At. Mol. Phys. **11** (1978) 1457.
5) V. V. Afrosimov, G. A. Leiko and M. N. Panov: Sov. Phys.-Tech. Phys. **25** (1980) 313.
6) M. B. Shah and H. B. Gilbody: J. Phys. B: At. Mol. Phys. **11** (1978) 121.
7) T. Kusakabe, H. Hanaki, N. Nagai, T. Horiuchi, I. Konomi and M. Sakisaka: Mem. Fac. Eng. Kyoto Univ. **45** (1983) 35.
8) H. Hanaki, N. Nagai, T. Kusakabe, T. Horiuchi and M. Sakisaka: Jpn. J. Appl. Phys. **22** (1983) 748.
9) K. H. Berkner, R. V. Pyle, J. W. Stearns and J. C. Warren: Phys. Rev. **166** (1968) 44.
10) M. B. Shah and H. B. Gilbody: J. Phys. B: At. Mol. Phys. **7** (1974) 256.
11) J. E. Bayfield and G. A. Khayrallah: Phys. Rev. A: **11** (1975) 920.
12) M. E. Rudd, T. V. Goffe and A. Itoh: Phys. Rev. A: **32** (1985) 2128.
13) G. R. Hertel and W. S. Koski: J. Chem. Phys. **40** (1964) 3452.
14) C. Harel and A. Salin: J. Phys. B: At. Mol. Phys. **13** (1980) 785.
15) M. Kimura: J. Phys. B: At. Mol. Opt. Phys. **21** (1988) L19.
16) A. F. Fergusson and B. L. Moiseiwitsch: Proc. Phys. Soc. **74** (1959) 457.
17) I. K. Fetisov and O. B. Firsov: Sov. Phys.-JETP **10** (1960) 67.
18) I. V. Komarov and R. K. Janev: Sov. Phys.-JETP **24** (1967) 1159.
19) M. I. Chibisov: Sov. Phys.-JETP **43** (1976) 879.
20) T. P. Grozdanov and R. K. Janev: J. Phys. B: At. Mol. Phys. **13** (1980) 3431.
21) M. Sakisaka, H. Hanaki, N. Nagai, T. Horiuchi, I. Konomi and T. Kusakabe: J. Phys. Soc. Jpn. **52** (1983) 716.
22) H. Hanaki, T. Kusakabe, N. Nagai and M. Sakisaka: J. Phys. Soc. Jpn. **52** (1983) 424.
23) T. Kusakabe, N. Nagai, H. Hanaki, T. Horiuchi and M. Sakisaka: J. Phys. Soc. Jpn. **52** (1983) 4122.